PFC/JA-91-4

ABSOLUTE VERSUS CONVECTIVE ANALYSIS OF INSTABILITIES IN SPACE PLASMAS

Abhay K. Ram and Abraham Bers

January 1991

Plasma Fusion Center
Massachusetts Institute of Technology
Cambridge, Massachusetts 02139 USA

This work was supported by NASA Grant No. NAGW-2048. Reproduction, translation, publication, use and disposal, in whole or part, by or for the United States Government is permitted.

Invited paper presented at the 1990 Cambridge Workshop on Theoretical Geoplasma Physics; to appear in *Physics of Space Plasmas (1990), SPI Conference Proceedings and Reprint Series, Number 10*, T. Chang, G. B. Crew, and J. R. Jasperse, eds. (Scientific Publishers, Cambridge, MA, 1991).

ABSOLUTE VERSUS CONVECTIVE ANALYSIS OF INSTABILITIES IN SPACE PLASMAS

Abhay K. Ram and Abraham Bers

TABLE OF CONTENTS

ABSTRACT

A brief description of the pinch-point analysis of the Green's function for studying the space-time evolution of instabilities in a homogeneous medium is presented. This analysis determines if an instability propagates in space-time as an absolute instability or as a convective instability. The pinch-point technique is applied to the study of electron cyclotron maser type of instabilities. Such instabilities are believed to be a source of some types of observed planetary, solar and stellar emissions, and, in particular, of auroral kilometric radiation. The pinch-point analysis also brings out the spectral differences between absolute and convective instabilities that should be important in correlating theoretical models with observations.

ABSOLUTE VERSUS CONVECTIVE ANALYSIS OF INSTABILITIES IN SPACE PLASMAS

Abhay K. Ram and Abraham Bers
Plasma Fusion Center, M.I.T., Cambridge, MA 02139

ABSTRACT

A brief description of the pinch-point analysis of the Green's function for studying the space-time evolution of instabilities in a homogeneous medium is presented. This analysis determines if an instability propagates in space-time as an absolute instability or as a convective instability. The pinch-point technique is applied to the study of electron cyclotron maser type of instabilities. Such instabilities are believed to be a source of some types of observed planetary, solar and stellar emissions, and, in particular, of auroral kilometric radiation. The pinch-point analysis also brings out the spectral differences between absolute and convective instabilities that should be important in correlating theoretical models with observations.

I. INTRODUCTION

Laboratory, Space, and Astrophysical plasmas are rich sources of electromagnetic radiation whose intensities are above the thermal levels of emission. There are two generic ways of generating this radiation. The first is due to some internal sources of free energy which excite, from noise, an instability inside the plasma. This occurs, for instance, due to spatial gradients or anisotropies inherent in the plasma. The second way that the plasma acts as a source of electromagnetic radiation is by stimulated scattering of some of the externally incident electromagnetic waves. This may happen when the incident waves couple nonlinearly to some normal modes of the plasma and unstably drive, from noise, the scattered radiation from inside the plasma. In either case, the instability evolves in the free energy source region leading, eventually, to electromagnetic radiation propagating out of the plasma.

An aspect of the radiation that is observed and measured by a detector or a probe, located in the source region or far away from it, is the intensity of the emission as a function of either the frequency or the wavelength of the emission. In order to understand the emission, one would like to know about the onset of the instability that leads to the observed emission, the propagation in space and time of the instability through the source region and beyond, and, finally, the evolution towards the saturated nonlinear state which is eventually observed. In this paper we are going to

discuss features of the linear evolution and propagation of instabilities in a homogeneous medium that would have distinguishable signatures in the observed spectra.

The linear evolution and propagation of instabilities in a homogeneous medium has been discussed before [1] . The essence of the Green's function technique used in these studies is presented in section II. In section III this technique is applied to the propagation of cyclotron maser type of instabilities. Such instabilities are considered to be a source of auroral kilometric radiation [2, 3]. The characteristic features associated with the propagation of such instabilities through space and time are also discussed in section III.

II. GREEN'S FUNCTION ANALYSIS OF INSTABILITIES

The propagation of a small amplitude signal in a homogeneous medium is described by an equation of the form:

$$\mathcal{L}\,\vec{\psi}(\vec{r},t) \;=\; \int d^3r' \int dt' \;\overline{\overline{M}}(\vec{r}-\vec{r'},t-t')\cdot\vec{\psi}(\vec{r'},t') \;+\; \vec{S}_{ext}(\vec{r},t) \quad (1)$$

where $\mathcal{L}$ is a linear operator, $\vec{\psi}$ is a vector function describing the small amplitude signal, $\overline{\overline{M}}$ describes the medium through which the signal is propagating, and $\vec{S}_{ext}$ is either a noise source or an external source acting on the medium. The space-time Fourier transform of the above equation yields:

$$\overline{\overline{D}}(\vec{k},\omega)\cdot\vec{\psi}(\vec{k},\omega) \;=\; \vec{S}_{ext}(\vec{k},\omega) \quad (2)$$

where $\overline{\overline{D}}$ is a sum of the Fourier transform of the left-hand side of Eq. (1) and the Fourier transform of $\overline{\overline{M}}$. If, for some real-$\vec{k}$, the corresponding ω's satisfying $det\left\{\overline{\overline{D}}(\vec{k},\omega)\right\} = D(\vec{k},\omega) = 0$ (where *det* denotes the determinant) are such that the imaginary part of ω is > 0, then the medium is considered to be unstable to a perturbation with that particular $\vec{k}$ and ω. Eq. (2) can be solved for $\vec{\psi}(\vec{k},\omega)$, so that the solution to Eq. (1) is given by:

$$\vec{\psi}(\vec{r},t) \;=\; \int_L \frac{d\omega}{2\pi} \int_F \frac{d^3k}{(2\pi)^3} \;\frac{\overline{\overline{D}}_{adj}(\vec{k},\omega)\cdot\vec{S}_{ext}(\vec{k},\omega)}{D(\vec{k},\omega)} \;\exp(i\vec{k}\cdot\vec{r}-i\omega t) \quad (3)$$

where $\overline{\overline{D}}_{adj}$ is the adjoint matrix of $\overline{\overline{D}}$, and L and F are the appropriate Laplace and Fourier contours of integration, respectively, which are chosen to satisfy causality [1].

While Eq. (3) gives the general space-time propagation of a signal in a medium driven by $\vec{S}_{ext}$, we are usually interested in the natural response of the medium. The Green's function technique gives a physical and general insight into the response properties of the medium [4]. The Green's function solution, $\vec{G}(\vec{r},t)$, is obtained by replacing $\vec{S}_{ext}$ in Eq. (1) by $\delta(\vec{r})\delta(t)\overline{\overline{I}}$, where $\overline{\overline{I}}$ is the identity tensor. The Green's function approach is equivalent to evaluating the response of the medium to a localized, broadband, "white" noise source. The response to a general perturbation is then obtained by convolving the Green's function with the perturbation [4].

In what follows, we shall consider scalar fields, ψ, and only one spatial dimension. For this case the Green's function is given by:

$$G(z,t) \;=\; \int_L \frac{d\omega}{2\pi} \int_F \frac{dk}{2\pi} \;\; \frac{1}{D(k,\omega)} \;\exp(ikz - i\omega t) \qquad (4)$$

where k is the wave-number in the z direction. The generalization to vector fields and higher spatial dimensions is more complicated but can be carried out in a straightforward manner.

Even for simple dispersion functions, $D(k,\omega)$, it is frequently difficult to compute the Green's function analytically. However, we are not generally interested in the transient solution to $G(z,t)$. Rather, we would like to know the time-asymptotic behavior of $G(z,t)$. It has been determined that, in an unstable medium, the time-asymptotic evolution of $G(z,t)$ can belong to one of only two possible categories [5, 6]:

(a) an *absolute instability*, where the response grows in time and encompasses more and more of the space as a function of time – the response always including the spatial location of the initial perturbation; thus, every spatial point eventually becoming unstable;

(b) a *convective instability*, where the response grows in time but propagates away from its point of origin; thus, any spatial point eventually becoming stable.

While the above classification of the time-asymptotic Green's function into two categories for an unstable medium is useful, it still leaves us with the daunting task of solving for $G(z,t)$ in the time-asymptotic limit. This task was considerably simplified by the "pinch-point" formalism that was originally put forth by Bers and Briggs [6, 7]. This formalism presented a convenient way to determine whether an unstable medium was absolutely unstable or convectively unstable, and, furthermore, completely determined the time-asymptotic Green's function. According to the pinch-point procedure, the time-asymptotic Green's function is completely determined by those k_o, ω_o which satisfy:

$$D(k_o,\omega_o) \;=\; 0\,, \qquad \frac{\partial D(k_o,\omega_o)}{\partial k} = 0 \qquad (5)$$

and are "pinch points". A pinch point is determined by the analytic continuation, in the complex ω-plane, of the Laplace contour, L, towards the real ω-axis [1, 7]. As L is lowered towards the real ω-axis the corresponding Fourier contour, F, is subsequently modified to satisfy causality. This is ensured by requiring that F does not intersect any branches obtained by the mapping of the L-contour into the complex k-plane through the dispersion relation: $D(k,\omega) = 0$. This condition is violated when two branches of the L-contour in the complex k-plane coming from opposite sides of the real k-axis meet and "pinch" the Fourier contour. This defines the pinch point in the complex k-plane and it requires that the Laplace contour be deformed past the corresponding (branch) point in the complex ω-plane (satisfying $D(k,\omega) = 0$). If a pinch point exists, and the corresponding point in ω is in the upper half plane at $\omega = \omega_0$, then the medium is absolutely unstable with the time-asymptotic form of the Green's function given by:

$$\lim_{t\to\infty} G(z,t)\Big|_{z=0} \sim \frac{1}{t^{1/2}} \exp(-i\omega_0 t) \tag{6}$$

Otherwise, the medium is convectively unstable.

The time-asymptotic form of $G(z,t)$ at the origin of the laboratory coordinate system ($z = 0$) is given by Eq. (6). The spatial form of $G(z,t)$ is obtained by doing the pinch-point analysis in all possible inertial frames which are moving with respect to the laboratory frame [6, 8]. In an inertial frame moving with velocity v with respect to the laboratory frame, the Green's function is given by:

$$G(z',t') = \int_{L'} \frac{d\omega'}{2\pi} \int_{F'} \frac{dk'}{2\pi} \frac{1}{D_v(k',\omega',v)} \exp(ik'z' - i\omega' t') \tag{7}$$

where the primed quantities are evaluated in the moving frame. D_v is given by:

$$D_v(k',\omega',v) = D\left[k(k',\omega',v),\omega(k',\omega',v)\right] \tag{8}$$

and the relation between the primed and the unprimed quantities is given by the Lorentz transformations:

$$\begin{aligned} z &= \gamma_v (z' + vt'), & t &= \gamma_v \left(t' + \frac{v}{c^2} z'\right), \\ k &= \gamma_v \left(k' + \frac{v}{c^2}\omega'\right), & \omega &= \gamma_v (\omega' + vk') \end{aligned} \tag{9}$$

where $\gamma_v = (1 - v^2/c^2)^{-1/2}$.

Then, as in Eq. (6), the time-asymptotic response of $G(z',t')$ at the origin of the primed coordinate system is:

$$\lim_{t'\to\infty} G(z',t')\Big|_{z'=0} \sim \frac{1}{(t')^{1/2}} \exp\{-i\omega_0'(v)t'\} \tag{10}$$

where the pinch point frequency in the primed coordinate system, $\omega_0'(v)$, is a function of the observer velocity. By using the transformation equations given in Eq. (9) it is easy to show that:

$$\lim_{t\to\infty} G(z,t)\Big|_{z=vt} \sim \left(\frac{\gamma_v}{t}\right)^{1/2} \exp\left\{-i\frac{\omega_0'(v)}{\gamma_v}t\right\} \tag{11}$$

Besides determining the spatial and temporal evolution of $G(z,t)$ in the time-asymptotic limit for an absolute instability, it is clear that this procedure also determines the spatial and temporal evolution of a convective instability.

Thus, from the pinch-point analysis the following properties of an unstable medium can be determined:

(a) the absolute versus convective nature of the unstable medium;

(b) the space-time evolution (*i.e.* the spatial and temporal growth rates) of a localized (at $z = 0$) noise source from an initial time to a time where the transient response of the system to the initial perturbations can be ignored;

(c) the velocity of propagation of the instability in the medium.

This last point is very important. In general, the velocity of propagation is not related to a group velocity of any mode satisfying the dispersion relation $D(k,\omega) = 0$. In particular, for an absolutely unstable medium the concept of a group velocity cannot be defined. Thus, ray-tracing in an absolutely unstable medium is meaningless.

It is important to note that the Green's function describes the natural responses of an infinitely extended medium. In contrast to responses in a bounded medium, this must entail that there be no (initial) excitations at infinity or, that, at infinity, the initial excitations decay faster than the space-time normal modes. If, at infinity, the initial conditions do not decay faster than the the space-time normal modes, it is meaningless to describe or distinguish the space-time evolution of these initial conditions in terms of the inherent properties of absolute and convective instabilities in that medium. By not paying attention to these mathematical details one can make misguided and misleading statements about the theory of absolute and convective instabilities [9].

III. SPACE-TIME EVOLUTION OF CYCLOTRON MASER TYPE OF INSTABILITIES

The cyclotron maser instability driven by a loss-cone distribution is believed to be a favorable explanation for the auroral kilometric radiation [2, 3], the Jovian decametric emission and similar emissions from Saturn and Uranus, certain types of continuum solar microwave bursts, and microwave emission from some flare stars [10]. In this section we consider a highly anisotropic, ring-like, electron distribution function in a uniform, background magnetic field and study the space-time evolution of instabilities propagating along the magnetic field [11–13]. Furthermore, we will use the pinch-point analysis to determine important characteristics that will help distinguish absolute instabilities from convective instabilities.

The electron distribution function is assumed to be of the form:

$$f_0(p_\perp, p_\parallel) = \frac{1}{2\pi p_{0\perp}} \delta(p_\perp - p_{0\perp})\, \delta(p_\parallel - p_{0\parallel}) \tag{12}$$

in a homogeneous magnetic field, $\vec{B}_0$. Here $p_\perp$ and $p_\parallel$ are the magnitude of the perpendicular (to $\vec{B}_0$) and parallel components of the momentum, respectively, and $\vec{p}_0$ is a constant momentum. Assuming the ions to be forming a cold, neutralizing background, the relativistic Vlasov equation leads to the following dispersion relation for right-handed circularly polarized electromagnetic waves propagating along $\vec{B}_0$:

$$\begin{aligned} D(k,\omega) = {} & (c^2k^2 - \omega^2) \left\{ (\omega - kv_\parallel - \omega_c)^2 + \frac{1}{2} \frac{v_\perp^2}{c^2} \omega_p^2 \right\} \\ & + \omega_p^2 (\omega - kv_\parallel)(\omega - kv_\parallel - \omega_c) \end{aligned} \tag{13}$$

where

$$v_\perp = \frac{p_{0\perp}}{\gamma_0 m_e}, \quad v_\parallel = \frac{p_{0\parallel}}{\gamma_0 m_e}, \quad \gamma_0 = \sqrt{1 + \frac{p_0^2}{m_e^2 c^2}}, \quad \omega_p = \frac{\omega_{p0}}{\sqrt{\gamma_0}}, \quad \omega_c = \frac{\omega_{c0}}{\gamma_0}$$

m_e is the electron rest mass, and ω_{p0} and ω_{c0} are the electron plasma and electron cyclotron frequencies, respectively, corresponding to the rest mass of the electrons. For $\omega_{p0}/\omega_{c0} = 0.2$, $v_\parallel = 0$ and $v_\perp = 0.2c$, the roots of the dispersion relation (real and imaginary parts of ω) are plotted in Fig. 1 as a function of real k. There are three branches of $D(k,\omega)$ corresponding to the whistler mode (whose phase velocity is less than the speed of light), an electromagnetic mode (whose phase velocity is greater than the speed of light) and a negative energy mode. The coupling of the

negative energy mode to the whistler mode or the electromagnetic mode leads to the whistler instability or the relativistic instability, respectively.

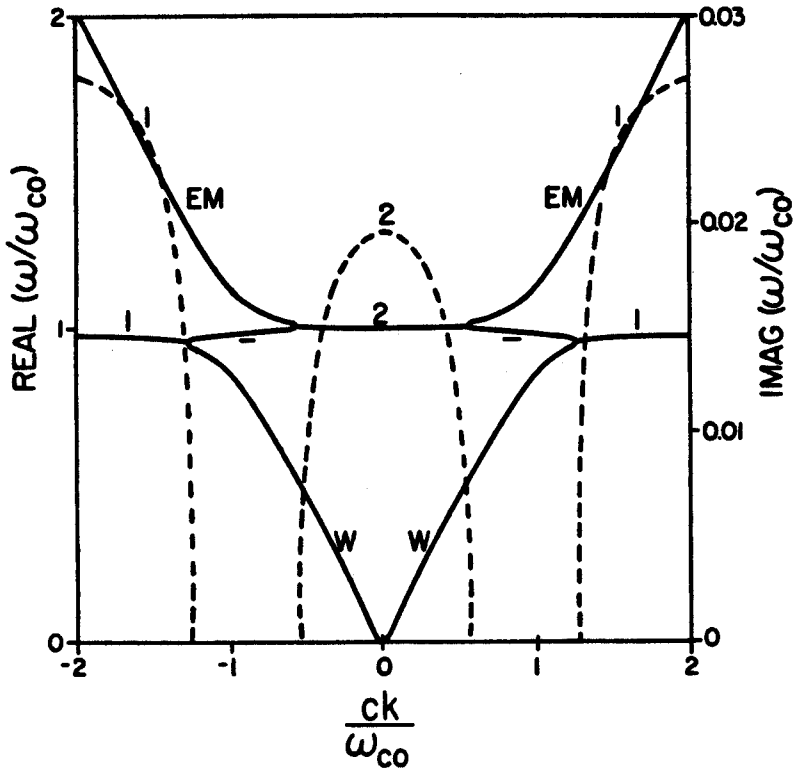

Figure 1. Real (solid line) and imaginary (dashed line) parts of the normalized frequency versus real, normalized wavenumbers. These are the roots of the dispersion function given in Eq. (13) for $\omega_{p0}/\omega_{c0} = 0.2$, $v_{\parallel} = 0$, and $v_{\perp} = 0.2c$. W is the whistler branch, EM is the electromagnetic branch, $-$ indicates the negative energy branch, 1 corresponds to the whistler instability and 2 to the relativistic instability.

For the parameters indicated above the pinch-point analysis in the laboratory frame shows that there are three pinch points with two of them corresponding to the whistler instability and one to the relativistic instability. The pinch points of the whistler instability are at $k_0 = \pm\infty$ and $\omega_0/\omega_{c0} \approx 0.98 + 0.028i$, while the pinch point of the relativistic instability is at $k_0 = 0$ and $\omega_0/\omega_{c0} \approx 0.999 + 0.02i$. Thus, the whistler and the relativistic instabilities are absolute instabilities with the whistler instability having a higher growth rate. The time-asymptotic form of the Green's function is determined by doing the pinch point analysis in all the iner-

tial frames moving with different velocities with respect to the laboratory frame. From Eq. (11):

$$\lim_{t\to\infty} \left| \ln\{G(z,t)\} \right|_{z=vt} \sim \frac{\omega'_{oi}(v)}{\gamma_v}\, t \tag{14}$$

where ω'_{oi} is the imaginary part of ω'_o. Here we have neglected the $\ln(t)$ term for large t. In Fig. 2 we have plotted the "pulse shape", *i.e.* $\omega'_{oi}(v)/\gamma_v$ as function of the observer velocity v. Since, in Fig. 2, the product of the abscissa with t gives z, and the product of the ordinate with t gives the right-hand side of Eq. (14), Fig. 2 gives the time-asymptotic, self-similar evolution of the magnitude of the logarithm of the Green's function.

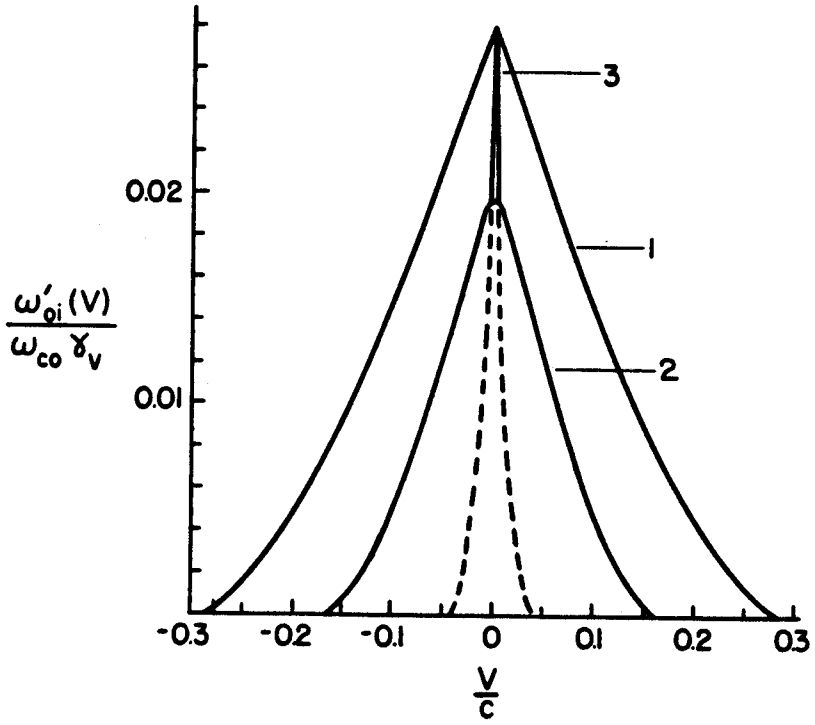

Figure 2. The appropriately normalized pulse shapes for the whistler (1,3) and the relativistic (2) instabilities. The parameters are the same as for Fig. 1. The dashed line indicates that the pinch point corresponding to 3 has been dissolved by 2. The pulse shapes for 1 and 2 are those of an absolute instability.

The two pinch points for the whistler waves (labeled 1 and 3 in Fig. 2), which have the same frequency at $v = 0$ (*i.e.* in the laboratory frame), become degenerate for $v \neq 0$. However, when $|v| \approx 0.005$, the whistler pinch point (3) interacts with the relativistic pinch point (labeled 2). Here,

the whistler pinch point (3) is "dissolved" [1] by the relativistic pinch point (2). Thereafter, for $|v| \gtrsim 0.005$, only the pinch points corresponding to the whistler instability (1) and the relativistic instability survive. In the rest of the discussion we shall consider only these two pinch points. From Fig. 2 the absolute nature of the two instabilities is quite clear.

The whistler instability, while it has a larger growth rate than the the relativistic instability, can be stabilized by thermal spreading of the ring distribution [12, 13]. The relativistic instability is not affected by thermal effects as its phase velocity is greater than the speed of light. So, instead of studying just the whistler instability, we shall also determine the behavior of the the relativistic instability.

In Eq. (11), the dominant variation of the Green's function in space and time is given by the exponential. The factor multiplying the exponential varies slowly with space and time. By neglecting this factor, the real part of the time-asymptotic Green's function is given by:

$$\Gamma(z,t) \;=\; \cos\left[\frac{1}{\gamma_v}\omega'_{or}(z/t)t\right]\;\exp\left[\frac{1}{\gamma_v}\omega'_{oi}(z/t)t\right] \qquad (15)$$

where, now, $\gamma_v = \left[1-(z/ct)^2\right]^{-1/2}$, and ω'_{or} is the real part of ω'_o. For an observer at a fixed point $z = z_o$, with $|z_o| > 0$, $\Gamma(z_o,t)$ gives the temporal history of an instability which has evolved from a broadband noise source located at $z = 0$ at time $t = 0$.

By the very nature of an absolute instability, $\Gamma(z_o,t)$ will continue to grow in time for all times. In Figs. 3a and 3b we have plotted the frequency spectrum of $\Gamma(z_o,t)$, *i.e.* $|\Gamma(z_o,\omega)|$, for the whistler and relativistic instabilities, respectively. The power spectrum is very narrow-band for both instabilities and the peak of the spectrum occurs near the laboratory pinch point frequency, $\omega'_{or}(v=0)$. Thus, to an observer in the unstable medium, the two absolute instabilities would correspond to very narrow frequency spectra.

As $v_{o\parallel}$ is increased, the maximum of the pulse shape occurs at an observer velocity $v = v_{o\parallel}$. For the same parameters as indicated above, the two instabilities become convective when $v_{o\parallel} \gtrsim 0.18c$. In order to illustrate the effect of relativity, and the characteristics of convective instabilities, we consider the case where $v_{o\parallel} = 0.85c$. The corresponding pulse shape is plotted in Fig. 4. Again, there are two pinch points corresponding to the whistler instability (labeled 1 and 3) and one pinch point for the relativistic instability (labeled 3). Pinch point 3 is dissolved by the relativistic instability and we are left with two pinch points (1 and 2). The pulse shape is highly asymmetric as compared to the pulse shape in Fig. 2. This asymmetry is due to the relativistic effects. It is clearly evident that the two instabilities are convective.

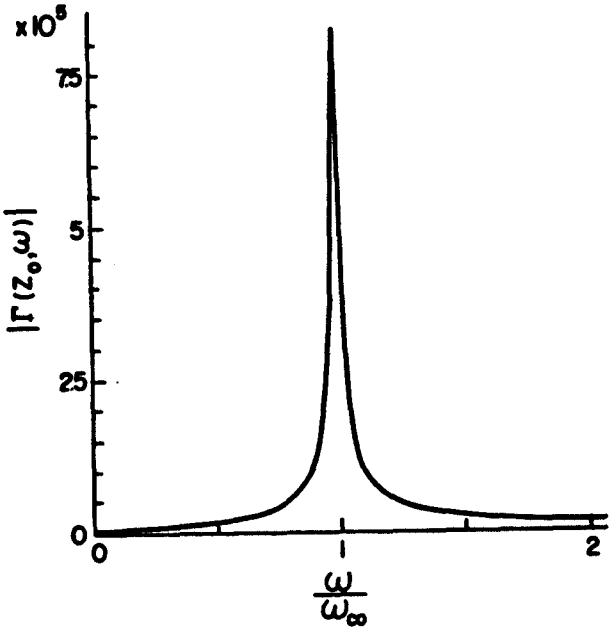

Figure 3a. The frequency spectrum of $\Gamma(z_0, t)$, with $z_0\omega_{c0}/c = 50$, for the whistler instability (labeled 1 in Fig. 2).

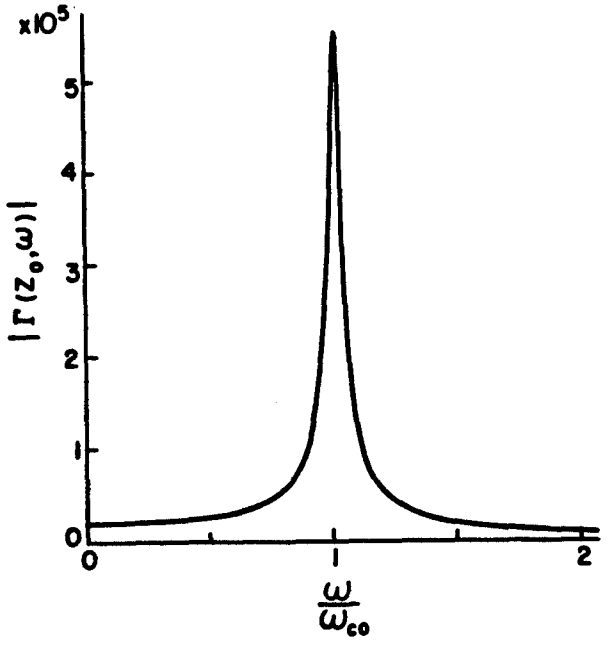

Figure 3b. The frequency spectrum of $\Gamma(z_0, t)$, with $z_0\omega_{c0}/c = 50$, for the relativistic instability (labeled 2 in Fig. 2).

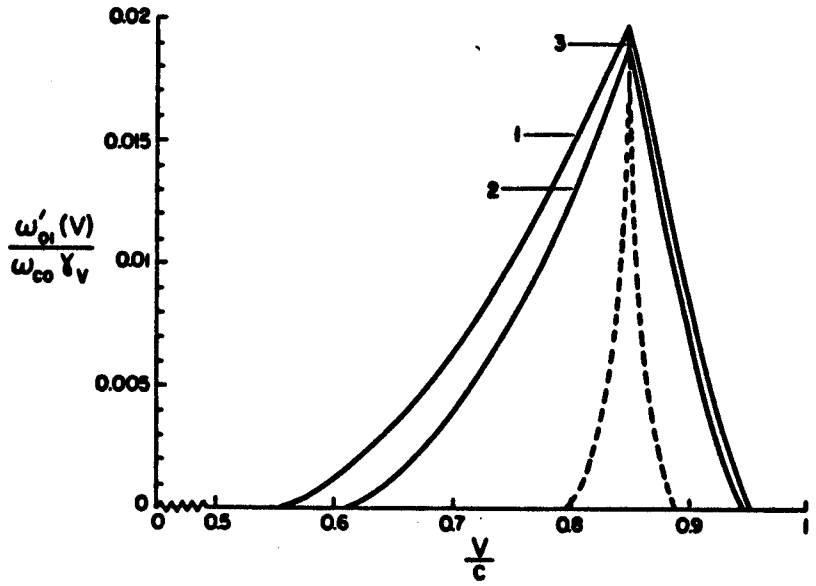

Figure 4. The appropriately normalized pulse shapes for the whistler (1,3) and the relativistic (2) instabilities. The parameters are the same as for Fig. 1 except that $v_{\parallel} = 0.85c$. Again, the pinch point corresponding to 3 has been dissolved by 2. The pulse shapes for 1 and 2 are those of a convective instability.

In order to calculate $\Gamma(z_0, t)$, the convective nature of the instabilities requires that the observer be at $z = z_0 > 0$. Furthermore, in contrast to an absolute instability where an observer sees a continuous growth of the signal, for the convective instability an observer will observe the instability for a finite amount of time. This is the case as shown in Figs. 5a and 5b for the whistler and the relativistic instabilities, respectively. The wave packet nature of the convective instability is obvious from these figures.

The power spectrum of the signal in Figs. 5a and 5b is plotted in Figs. 6a and 6b, respectively. The relative broadband nature of the spectrum, as compared to the case when the whistler and relativistic instabilities were absolute, is clearly evident. The power is spread out to harmonics of the electron cyclotron frequency.

Thus, there is a distinct observational difference between absolute and convective instabilities. The emission corresponding to an absolute instability will have a narrow frequency spectrum while a convective instability will correspond to a broadband emission.

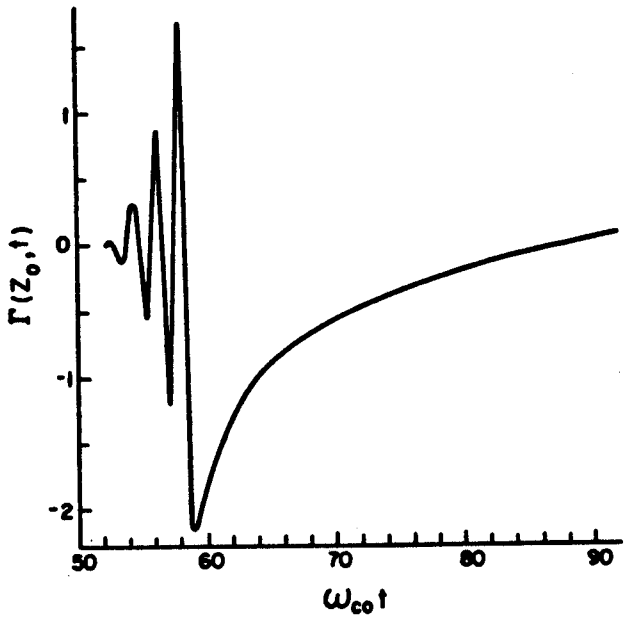

Figure 5a. $\Gamma(z_0,t)$, with $z_0\omega_{co}/c = 50$, as a function of the normalized time for the whistler instability (1 in Fig. 4).

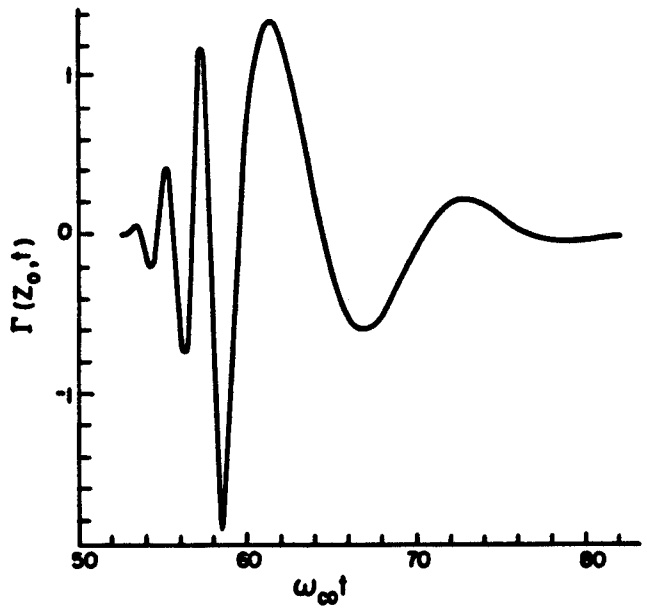

Figure 5b. $\Gamma(z_0,t)$, with $z_0\omega_{co}/c = 50$, as a function of the normalized time for the relativistic instability (2 in Fig. 4).

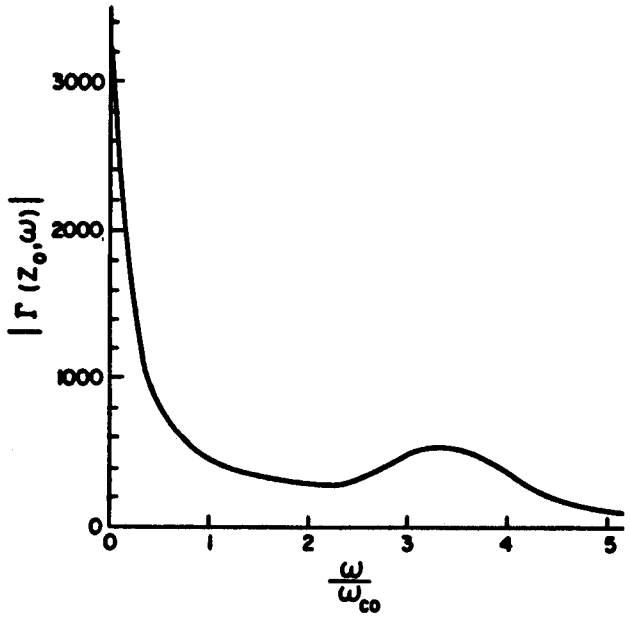

Figure 6a. Frequency spectrum of the $\Gamma(z_0, t)$ shown in Fig. 5a.

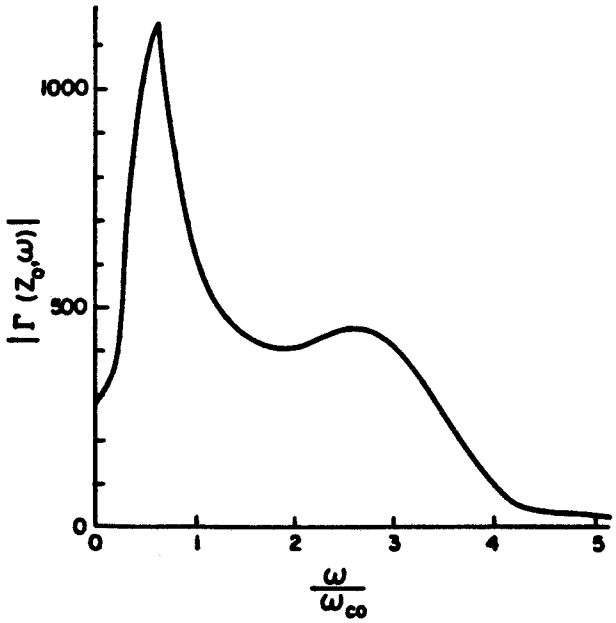

Figure 6b. Frequency spectrum of the $\Gamma(z_0, t)$ shown in Fig. 5b.

We have also done a pinch-point analysis for electromagnetic instabilities propagating across $\vec{B}_0$ that are generated by a ring distribution function of electrons. We have studied those instabilities whose phase velocities are greater than the speed of light and, thus, are not affected by cyclotron resonance damping. Furthermore, we have restricted ourselves to the case of $\omega_{p0}/\omega_{c0} << 1$ (which is an appropriate limit for the conditions that exist in the source regions of the auroral kilometric radiation). Instabilities are generated near the electron cyclotron frequency and its harmonics. We observe an interesting space-time behavior of these instabilities as a function of ω_{p0}/ω_{c0}. For very small densities ($\omega_{p0}/\omega_{c0} \approx 0.05$ with $v_\parallel = 0$ and $v_\perp = 0.1c$) the instability near the fundamental electron cyclotron frequency is an absolute instability while the instabilities at the harmonics are convective instabilities. As ω_{p0} is increased the instability at the second harmonic also becomes an absolute instability. For further increases in ω_{p0} ($\omega_{p0}/\omega_{c0} \approx 0.25$) the instability at the fundamental cyclotron frequency becomes convective while the instability at the second harmonic remains as an absolute instability. Hence, we have harmonic generation from a completely linear theory. These results should be important in explaining the observed emission at harmonics of the electron cyclotron frequencies in the auroral regions [14]. Details of all the results on the propagation of instabilities across the magnetic field will be published elsewhere.

CONCLUSIONS

A pinch-point, Green's function analysis of electron cyclotron maser instabilities has been shown to yield observationally interesting features about the space-time propagation of such instabilities. An absolute instability is found to have a narrow-band frequency spectrum while a convective instability has a broadband frequency spectrum. This feature should be important in correlating experimental observations with theoretical models.

Although, no mention has been made of the nonlinear saturation mechanisms for these instabilities, it is evident from some previous results [1] that the nonlinearly saturated state of an absolute instability is very different from that of a convective instability. In general, observed emissions are from nonlinearly saturated states of instabilities that have evolved in either an absolute or a convective manner in their linear stage. These nonlinear states can be expected to carry signatures of whether, linearly, the instability was of an absolute type or a convective type. This aspect needs to be accounted for when modeling experimental observations.

ACKNOWLEDGEMENTS

This work was supported by NASA Grant No. NAGW-2048.

REFERENCES

[1] A. Bers, *Handbook of Plasma Physics*, Vol. 1, M. N. Rosenbluth, and R. Z. Sagdeev, eds. (North-Holland, Amsterdam 1983), Chap. 3.2.
[2] D. B. Melrose, Astrophys. J. **207**, 651 (1976).
[3] C. S. Wu and L. C. Lee, Astrophys. J. **230**, 621 (1979).
[4] P. M. Morse and H. Feshbach, *Methods of Theoretical Physics* (McGraw-Hill, New York 1953).
[5] L. D. Landau and I. M. Lifshitz, *Electrodynamics of Continuous Media* (in Russian, GITTL, Moscow 1953); see also their *Fluid Mechanics* (Pergamon Press, London 1959).
[6] See Ref. [1] above and references therein.
[7] R. J. Briggs, *Electron-Stream Interaction with Plasmas* (MIT Press, Cambridge, MA 1964).
[8] A. Bers, A. K. Ram, and G. Francis, Phys. Rev. Lett. **53**, 1457 (1984).
[9] T. E. Oscarsson and K. G. Rönnmark, Geophys. Res. Lett. **13**, 1384 (1986). A detailed discussion of the misconceptions in this paper will be presented in a forthcoming publication.
[10] C. S. Wu, Space Sci. Revs. **41**, 215 (1985) and references therein.
[11] V. V. Zhelezniakov, Izv. Vys. Voch. Zaved. Radiofiz. **2**, 14 (1959).
[12] A. Bers, J. K. Hoag, and E. A. Robertson, Quart. Prog. Reports No. 77, pp. 149-152; No. 78, pp. 105-110; No. 79, pp. 107-112, Res. Lab. of Electronics, MIT, Cambridge, MA (1965).
[13] A. K. Ram, G. Francis, and A. Bers, Proceedings of the Fourth International Workshop on Electron Cyclotron Emission and Electron Cyclotron Resonance Heating (Ufficio Edizioni Scientifiche, Frascati, Rome, Italy 1984); and M.I.T. Plasma Fusion Center Report PFC/CP-84-5, Cambridge, MA (1984).
[14] R. F. Benson, J. Geophys. Res. **90**, 2753 (1985).